Chemical Engineering Journal 95 (2003) 15–24

Chemical Engineering Journal

www.elsevier.com/locate/cej

Separate/simultaneous catalytic reduction of sulfur dioxide and/or nitric oxide by carbon monoxide over titanium–tin solid solution catalysts

Zhang Zhaoliang [a,b,*], Ma Jun [a], Yang Xiyao [a]

[a] *Catalysis Division, College of Chemistry and Molecular Engineering, Peking University, Beijing 100081, PR China*

[b] *Hainan Liuhe Environmental Protection Catalysts Co. Ltd., Jinniu Road, Jinpan Industry Development Zone, Haikou 570216, PR China*

Received 25 September 2002; accepted 22 February 2003

Abstract

Titanium–tin solid solutions prepared by coprecipitation were studied for the separate and simultaneous catalytic reduction of SO_2 and/or NO by CO. Physicochemical characterizations of the solid solutions before and after reactions with different SnO_2 contents were conducted to disclose the reaction mechanism by means of XRD, CO–TPR, XPS and transient MS techniques. It is found that TiO_2–SnO_2 solid solutions were very active towards the reduction of SO_2 by CO at a low temperature and space velocity. There existed a strong synergistic promoted effect, which can be explained based on an enhanced redox mechanism proposed in the work. Furthermore, TiO_2–SnO_2 solid solutions would show a pronounced increase in catalytic activity during the reduction of NO by CO after the catalysts finished $SO_2 + CO$ reactions, or by introducing SO_2 into the reaction feed. This promoting effort is due to the formation of tin sulfide species as a product of the reduction of SO_2 by CO on the catalyst surface. A NO decomposition mechanism with the formation of SO_2 by-product was proposed. The produced SO_2 was in situ catalytically reduced to sulfur to regenerate tin sulfide. Lastly, simultaneous catalytic reduction of SO_2 and NO using CO as a reducing agent was carried out on TiO_2–SnO_2 solid solution catalysts. Experimental results showed that at a temperature above 350 °C, SO_2 and NO conversions are greater than 91 and 99%, respectively.

Keywords: SO_2; NO; CO; Catalytic reduction; Tin dioxide; Titania; Solid solution

1. Introduction

Sulfur dioxide (SO_2), nitric oxide (NO) and carbon monoxide (CO) are three major air pollutants. They are usually emitted as by-products of combustion processes from industrial, transportation and domestic activities and, in many occasions, simultaneously. Various processes are now under operation or research to remove SO_2 and NO separately or simultaneously [1]. The catalytic reduction of SO_2 by CO to valuable sulfur is desirable as CO is then simultaneously removed from the flue gas. Furthermore, the process is single-staged and easy to design and operate. Several types of active catalysts have been investigated. Early developed are alumina-supported transition metals and oxides [2,3], however, production of COS, which is much more harmful than SO_2, usually proceeds to a substantial extent on these catalysts. The COS formation could be lowered by using the perovskite $LaTiO_3$ [4], and even completely removed over $La_{0.7}Sr_{0.3}CoO_3$ catalyst [5]. Unfortunately, the perovskite-type catalysts lost their structure under reaction conditions and turned into a complex mixture of sulfides and oxysulfides which act as active phases [6]. Recently Ma et al. [7,8] reported that La_2O_2S is an effective catalyst for this reaction. Over 98% SO_2 conversion and selectivity to elemental sulfur can be achieved above 500 °C. Irrespective of the high reaction temperature, the synthesis of La_2O_2S is difficult and complex [9]. Mixed oxides of Co_3O_4–TiO_2 [10] and Al_2O_3 supported sulfides of transition metals [11] were also reported to be active and selective catalysts, but both of them need sulfurization pretreatment in order to get the active phase. As all above are sulfide-based catalysts, which can be explained by a COS intermediate mechanism, more or less COS will be released inevitably in the course of the reaction. Flytzani-Stephanopoulos and co-workers [12–14] reported the activity of ceria-base complex oxides for the reduction of SO_2 by CO at high space velocity and in the presence of low amounts of H_2O. Although the catalyst structure is maintained during the reaction, the temperature of SO_2 complete removal is relatively high.

The removal of NO has been extensively studied in recent years for environmental protection. NO reduction by CO is one of the fundamental reactions in the presence of CO,

* Corresponding author.
E-mail address: zhangzhaoliang@sdu.edu.cn (Z. Zhaoliang).

1385-8947/$ – see front matter
doi:10.1016/S1385-8947(03)00061-5

especially for so-called three-way automotive catalysts (TWC). This reaction has been studied over noble metals [15–17], transition metals [18,19], perovskites [20,21] and mixed oxides [22]. However, few works have been concerned with the effects of SO_2 on the reaction. In respect that fuels contain residual sulfur, any practical catalyst needs to be resistant to SO_2. In general, SO_2 is thought to be the most important poison for lean NO_x catalysts because of competing adsorption on the active sites of the catalyst with nitrogen oxide [23]. For instance, Gandhi and Shelef [24] found that the activity of NO reduction to N_2 over the γ-Al_2O_3 supported Pt and Pd catalyst was completely suppressed by the presence of very low levels of SO_2.

As to the simultaneous removal of SO_2 and NO, wet lime/limestone scrubbers for desulfuration and selective catalytic reduction of nitrogen oxides with NH_3 have been commercialized [25], but the combination processes are complicated and produce sufficient amount of solid/liquid wastes that require further disposal. Therefore, the dry type sorbent/catalyst process for simultaneous removal of SO_2 and NO was developed [26–28]. Because SO_2 is oxidized to SO_3 and then fixed on the catalysts as sulfates in the process, the sulfated catalyst must be periodically removed for regeneration and repeated use. In these regards, direct catalytic reduction of SO_2 and NO to elemental sulfur and N_2, respectively, by CO in a one-way process has been under development. Kittrell and co-workers [29–31] reported alumina-supported transition metals were effective catalysts. Besides the catalysts needing to be activated by introducing a gas containing CO and SO_2, substantial amounts of undesirable COS formed are required to be eliminated in another catalyst bed. Other sulfide-based catalysts, for example, La_2O_2S–CoS_2 [32] and $CoMo/Al_2O_3$ [33] have also been reported. Again, these catalysts must be pre-sulfidized as in the case of separate reduction of SO_2 by CO. Ceria-based catalysts [14], which show 77% sulfur yield and 100% NO conversion at 550 °C in the presence of high content of water, seem to be promising except for the high reaction temperature.

Tin oxide-based catalysts have been known for a long time to have a good activity towards the oxidation of CO and the reduction of NO by CO [34]. Bulk [35] and alumina supported SnO_2 [36,37] have shown good activities in the selective catalytic reduction of NO by hydrocarbons. On the other hand, rutile TiO_2 is observed to be active in the reduction of SO_2 by CO at high temperatures [10]. Moreover, TiO_2 is also a better support and catalyst than Al_2O_3 in the Claus reaction for its more resistance to the sulfation reaction [38].

In a short communication [39], we firstly reported that TiO_2–SnO_2 solid solutions were much more active catalysts for the simultaneous catalytic reduction of SO_2 and NO by CO to their respective elements and the activity of the catalytic reduction of NO by CO was greatly improved when SO_2 was added, which is often thought to be a poison to the catalyst. In this paper, the detailed results will be shown, and especial attention is focused on the mechanism aspects of the reaction systems.

2. Experimental

2.1. Catalyst preparation

$Ti_{1-x}Sn_xO_2$ ($x = 0.05$, 0.12, 0.35, 0.68) solid solutions, corresponding to the mass ratio of TiO_2 and SnO_2 of 9:1, 4:1, 1:1 and 1:4, were prepared by coprecipitation method. The stoichiometric mixed solution of $Ti(SO_4)_2$ and $SnCl_4{\cdot}5H_2O$ together with the solution of ammonia were simultaneously dropped into de-ionized water under vigorous agitation, and then the solution was aged for 30 min. The resultant precipitates were dried at 120 °C overnight and calcined at 500 °C for 5 h in air. For comparison, pure TiO_2 and SnO_2 were also prepared by the same procedures mentioned above, and by using one of the precursors.

2.2. Reaction studies

A U-shaped quartz reactor (i.d. = 6 mm) with a porous quartz frit supporting the catalyst was used for reaction tests under atmospheric conditions. The model flue gases employed are shown in Table 1. The total flow rate was 40 cm^3/min, and 1 g of catalyst was paced in the reactor leading to a space velocity of 2400 h^{-1}. The products in the effluent stream were analyzed by an online quadrupole mass spectrometry (LZL-204, Beijing Analytical Instrument Plant). The SO_2 and NO conversions were calculated on the basis of the differences between the inlet and

Table 1
Typical SO_2 and NO compositions of flue gas emitted from combusting coal with sulfur of 1–3 wt.% and model flue gas employed, GHSV = 2400 h^{-1}, balance gas Ar

Components	Actual flue gas [40] (vol.%)	Feed compositions employed (vol.%)		
		Separate reduction of SO_2 by CO to S	Separate reduction of NO by CO to N_2	Simultaneous reduction of SO_2 and NO to S and N_2
SO_2	200×10^{-4}–2000×10^{-4}	1050×10^{-4}	–	525×10^{-4}
NO	200×10^{-4}–2000×10^{-4}	–	1025×10^{-4}	520×10^{-4}
CO		2085×10^{-4}	2085×10^{-4}	2085×10^{-4}

outlet SO_2 and NO intensities, respectively. The data for steady-state activity of the catalysts were collected after 2 h testing.

2.3. Catalyst characterization

X-ray powder diffraction (XRD) patterns were recorded on a Rigaku D/max 2000 diffractmeter employing Cu Kα radiation.

The BET specific surface area was measured by a Micromeritics ASAP-2010 instrument.

X-ray photoelectron spectroscopy (XPS) analyses were performed with a VG ESCALAB5 system.

CO–TPR experiments were conducted on the same catalytic apparatus at a heating rate of 10 °C/min in a flow of 4170×10^{-4} vol.% CO in Ar.

The transient response technique is also used to elucidate the reaction mechanism. First, Ar flowed through the catalyst at the desired temperature, and the concentration step change Ar/NO + Ar, Ar/NO + CO + Ar, was then enforced by switching a four-way valve.

The mass-to-charge (*m*/*e*) ratios were monitored by MS as follows: SO_2 (64), NO (30), CO and N_2 (28), CO_2 and N_2O (44), NO_2 (46), COS (60).

3. Results

3.1. Catalytic activity

3.1.1. Separate reduction of SO_2 by CO

Fig. 1 shows the conversion of SO_2 and the selectivity towards elemental sulfur as a function of reaction temperature over the solid solutions. Both $Ti_{0.65}Sn_{0.35}O_2$ and $Ti_{0.88}Sn_{0.12}O_2$ catalysts exhibit a complete removal of SO_2 with negligible COS formation at 350 °C, which is remarkable among the non-presulfied catalysts considering that the boiling point of elemental sulfur is 444.6 °C. Although $Ti_{0.95}Sn_{0.05}O_2$ catalyst shows excellent selectivity towards S, its activity is low below 400 °C. More tin in the solid solutions, i.e. $Ti_{0.32}Sn_{0.68}O_2$ will result in low values of both the conversion and selectivity.

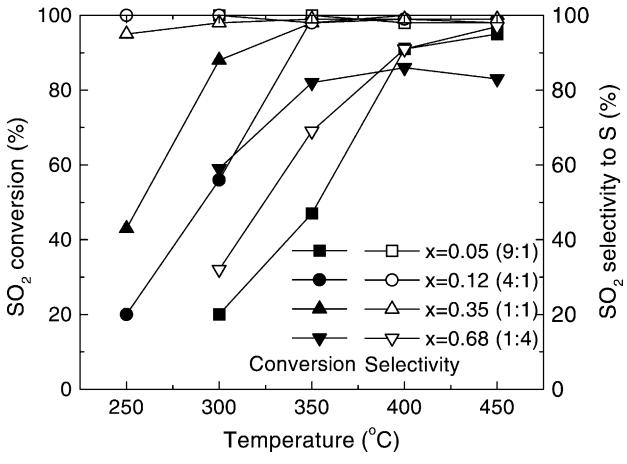

Fig. 1. SO_2 conversion and selectivity towards elemental S in the SO_2+CO reaction over $Ti_{1-x}Sn_xO_2$ solid solutions. Reaction conditions are described in Table 1.

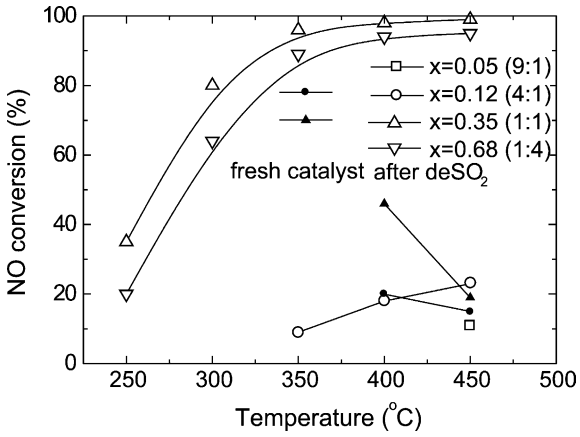

Fig. 2. NO conversion in the NO + CO reaction over $Ti_{1-x}Sn_xO_2$ solid solutions before and after finishing SO_2 + CO reactions. Reaction conditions are described in Table 1.

3.1.2. Separate reduction of NO by CO

Fig. 2 shows NO conversion for the reaction of NO + CO as a function of reaction temperature on $Ti_{1-x}Sn_xO_2$ solid solutions before (fresh catalyst) and after finishing SO_2 + CO reactions (deSO_2). It is found that both fresh $Ti_{0.95}Sn_{0.05}O_2$ and $Ti_{0.32}Sn_{0.68}O_2$ catalysts do not show any catalytic activity in the whole temperature range. However, after deSO_2 reactions, the $Ti_{0.95}Sn_{0.05}O_2$ catalyst is slightly active at 450 °C. Surprisingly $Ti_{0.32}Sn_{0.68}O_2$ catalyst shows a pronounced increase in catalytic activity. The same increase is also observed for $Ti_{0.65}Sn_{0.35}O_2$ catalyst: NO conversion is nearly 100% above 350 °C. Generally there is a tread of increased activity as the tin content increases. However, excess tin is not necessary to get high NO conversion. For example, the $Ti_{0.32}Sn_{0.68}O_2$ catalyst showed slightly lower activity than the $Ti_{0.65}Sn_{0.35}O_2$ catalyst. It is also noticed that NO conversions showed a decrease from 400 to 450 °C over fresh catalysts, while after they finished SO_2 + CO reactions, a monotonic increase was observed for all samples. These results indicate that the NO + CO reaction over the catalyst after deSO_2 reactions has a dependence on tin and a completely different mechanism from the fresh catalyst. Finally, it should be pointed out that the reduction of NO by CO over fresh $Ti_{1-x}Sn_xO_2$ solid solutions below 350 °C is unstable with reaction time. Therefore, none but conversions at 400 and 450 °C of fresh $Ti_{0.88}Sn_{0.12}O_2$ and $Ti_{0.65}Sn_{0.35}O_2$ catalysts were present in Fig. 2. This will be discussed further thereafter.

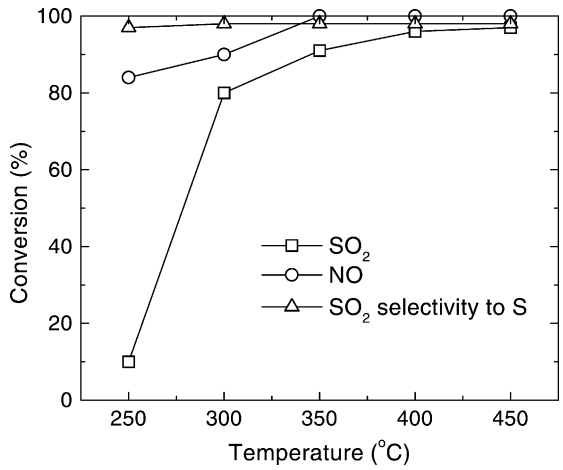

Fig. 3. SO_2, NO conversions and SO_2 selectivity towards elemental sulfur in the $SO_2 + NO + CO$ reaction over the $Ti_{0.65}Sn_{0.35}O_2$ catalyst. Reaction conditions are described in Table 1.

3.1.3. Simultaneously catalytic reduction of SO_2 and NO by CO

On the basis of above findings, simultaneous reduction of SO_2 and NO by CO over the $Ti_{0.65}Sn_{0.35}O_2$ catalyst is conducted. Fig. 3 shows the conversions of SO_2 and NO and SO_2 selectivity towards sulfur as a function of reaction temperature. Almost complete NO conversion and more than 91% SO_2 conversion can be achieved at 350 °C. The SO_2 selectivity towards S is kept above 97% even at the temperature as low as 250 °C. Similar results were also observed on $Ti_{0.32}Sn_{0.68}O_2$ catalyst. At 400 °C, SO_2 and NO conversions were 85 and 92%, respectively, but SO_2 selectivity to sulfur was only 86%.

3.2. Characteristics

3.2.1. XRD analysis

The XRD patterns of the fresh $Ti_{1-x}Sn_xO_2$ solid solutions calcined at 500 °C for 5 h were shown in Fig. 4. All samples were found to be the rutile structure of pure SnO_2 except for pure TiO_2, which is identified the anatase structure. However, the SnO_2 reflections were shifted to a higher angle (2θ) with the increasing amount of TiO_2. Table 2 presents the lattice parameters, cell volume, and specific surface areas of $Ti_{1-x}Sn_xO_2$ solid solutions. It is very obvious that the lattice parameters and cell volume of the solid solutions decreased with TiO_2 contents in accord with Vegard's law, as shown in Fig. 5. The broad peaks arose from their poor crystallinity and fine particle size. For instance, the crystallinity of $Ti_{0.95}Sn_{0.05}O_2$ sample was only about 59%. From the analysis of the X-ray line broading, using the Scherrer formula, it is also found that the particle sizes of all samples were of nanometer scale. This is in good agreement with their high specific surface areas.

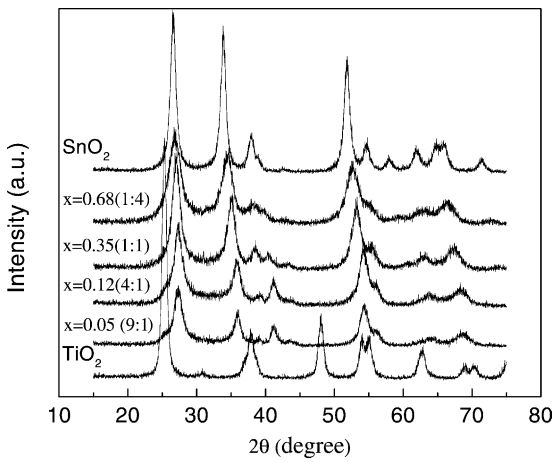

Fig. 4. XRD patterns of $Ti_{1-x}Sn_xO_2$ solid solutions calcined at 500 °C for 5 h.

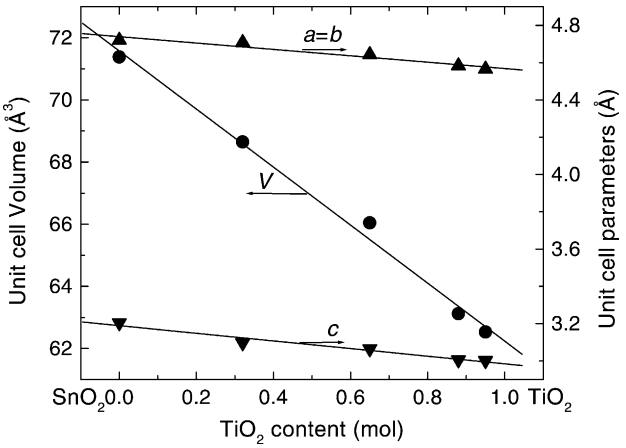

Fig. 5. Variation of lattice parameters a and c and unit cell volume V for $Ti_{1-x}Sn_xO_2$ solid solutions calcined at 500 °C for 5 h.

The XRD patterns of the used $Ti_{1-x}Sn_xO_2$ solid solutions were also checked (not shown here). No differences were detected between the fresh and used ones, which indicated that the catalysts were stable in the present reaction conditions.

3.2.2. CO–TPR

Fig. 6 presents the consumption of CO and the resulting production of CO_2 during TPR with 4170×10^{-4} vol.% CO in Ar over pure TiO_2, SnO_2 and $Ti_{0.65}Sn_{0.35}O_2$ solid solution. For anatase TiO_2, little activity towards the oxidation of CO was observed, in agreement with previous work [41]. However, SnO_2 showed activity above 100 °C. As to the $Ti_{0.65}Sn_{0.35}O_2$ solid solution, great CO consumption was not noticed until temperature increased above 225 °C, beyond which there was a sudden consumption of CO with concomitant production of CO_2. So the redox property of the TiO_2–SnO_2 solid solutions has been modified substantially compared with pure TiO_2 and SnO_2.

3.2.3. XPS analysis

Fig. 7 shows the XP spectra of the fresh and used (after $deSO_2$ and after $deSO_2$ + deNO + $deSO_2$ − NO) $Ti_{0.65}Sn_{0.35}O_2$ catalysts. On the fresh catalyst, the binding

Table 2
Lattice parameters, cell volume and surface area of $Ti_{1-x}Sn_xO_2$ solid solutions

$Ti_{1-x}Sn_xO_2$	TiO_2:SnO_2 (weight ratio)	$a = b$ (Å)	c (Å)	Cell volume (V) (Å^3)	Surface area ($m^2\,g^{-1}$)
TiO_2 (A)	1:0	4.594[a]	2.958[a]	62.428[a]	104
$Ti_{0.95}Sn_{0.05}O_2$	9:1	4.565	3.001	62.530	99
$Ti_{0.88}Sn_{0.12}O_2$	4:1	4.583	3.005	63.117	84
$Ti_{0.65}Sn_{0.35}O_2$	1:1	4.643	3.064	66.045	90
$Ti_{0.32}Sn_{0.68}O_2$	1:4	4.708	3.097	68.646	108
SnO_2	0:1	4.720	3.204	71.380	36

[a] Calculation from standard rutile date.

Table 3
Surface composition analysis of the $Ti_{0.65}Sn_{0.35}O_2$ catalyst by XPS

Atomic ratio	Sn/Ti	S/Sn
Bulk material[a]	0.538	–
Fresh catalyst	0.563	–
After $deSO_2$	0.705	0.102
After $deSO_2$ + deNO + $deSO_2$ − NO	0.762	0.028

[a] Based on stoichiometry.

energy of Sn $3d_{5/2}$ was 485.5 eV, which is between the values of those in SnO_2 or SnO (486.4 eV) and elemental Sn (484.7 eV) [42], suggesting a high oxygen deficiency state, for example, SnO_{2-x} on the catalyst surface [43]. However, the Sn 3d core levels show a slight increase on the catalyst after $deSO_2$ reaction. The Sn $3d_{5/2}$ peak at 486.4 eV has been assigned to SnO_2, SnO and SnS_2 [44]. This was also confirmed by the double S 2p XP spectra, which indicated two kinds of sulfur: metal sulfide (SnS_2) and sulfite ($SnSO_3$) [45] contributing to the low (161.4 eV) and high (168.3 eV) binding energy values, respectively. But, the later contains so little that its characteristic peak of oxygen at 533.3 eV [46] cannot be seen on O 1s profile of the used catalysts. Ti 2p for both fresh and used catalysts is similar to bulk TiO_2. In comparison with the catalyst after $deSO_2$ reaction, no significant variations of the spectra of Sn 3d and S 2p were observed for the catalyst after $deSO_2 + deNO + deSO_2 - NO$ reaction. The qualitative surface compositional analysis of the $Ti_{0.65}Sn_{0.35}O_2$ catalyst by XPS is given in Table 3. The atomic ratio of Sn/Ti on fresh catalyst was about 0.563, appropriately in agreement with the theoretical ratio. This suggests that the Sn/Ti ratio of the surface is equal to that of the bulk. However, after use the surface was enriched of Sn. The S/Sn ratios after $deSO_2$ and $deSO_2 + deNO + deSO_2 - NO$ reactions were also shown in Table 3.

4. Discussion

Tin and titanium dioxides crystallize in tetragonal symmetry with two molecules per unit cell and form solid solutions over the entire composition range. Both components show n-type semiconductivity induced by oxygen-deficient defect structures. However, because of the slight difference in radius between the Sn^{4+} cation (0.71 Å) and the Ti^{4+} cation (0.68 Å), the SnO_2 lattice is somewhat larger than that of TiO_2, as evidenced by the lattice parameters: $a = 4.7380$ Å and $c = 3.1865$ Å for SnO_2 and $a = 4.5941$ Å and $c = 2.9589$ Å for TiO_2 [47]. Furthermore SnO_2 and TiO_2 also exhibit rather different surface properties: Ti cations act as Lewis acid sites, whereas the removal of oxygen from SnO_2 leading to the formation of surface Sn^{2+} is expected to inhibit the acid–base interaction [48]. Therefore, the solid solutions will behave differently from the single oxides and composition changes. Recently, TiO_2–SnO_2 solid solutions have been paid much attention as attractive materials for gas sensors [49] because of its excellent electronic conductivity and oxygen ion mobility. In this work, we reported their new application in environmental catalysis, namely the removal of sulfur dioxide (SO_2), nitric oxide (NO) and carbon monoxide (CO).

The rutile form of pure TiO_2 normally exists only at temperatures above 700 °C, thus XRD patterns in Fig. 4 show that pure TiO_2 calcined at 500 °C was anatase, but the addition of small proportions of SnO_2 favors the transformation of anatase to rutile [50]. This indicated the formation of more oxygen vacancies in $Ti_{1-x}Sn_xO_2$ solid solutions (41). While oxygen vacancy and mobility are thought to be important properties for the reduction of both SO_2 [12] and NO [51] by CO.

Because anatase TiO_2 is a poor catalyst for thermal oxidation of carbon monoxide, as shown in CO–TPR spectrum, it is easy to understand that it has negligible activity for the reduction of SO_2 or NO by CO throughout the temperature range of the experiment. However, rutile TiO_2 may react with CO producing CO_2 beyond 400 °C during CO–TPR, consequently, showing activity in the SO_2 + CO reaction above 400 °C and a sharp rise with temperature increase [10]. Considering SnO_2 is much active for CO oxidation [52], the inactive result for the reduction of SO_2 by CO seems to be amazing. In fact, as mentioned above, Sn^{4+} tends to be reduced to Sn^{2+} in the presence of CO [48,53], and thus lost its activity.

4.1. SO_2 + CO reaction mechanism

According to the above discussions on pure TiO_2 or SnO_2 and catalytic activity results of the solid solutions, it is

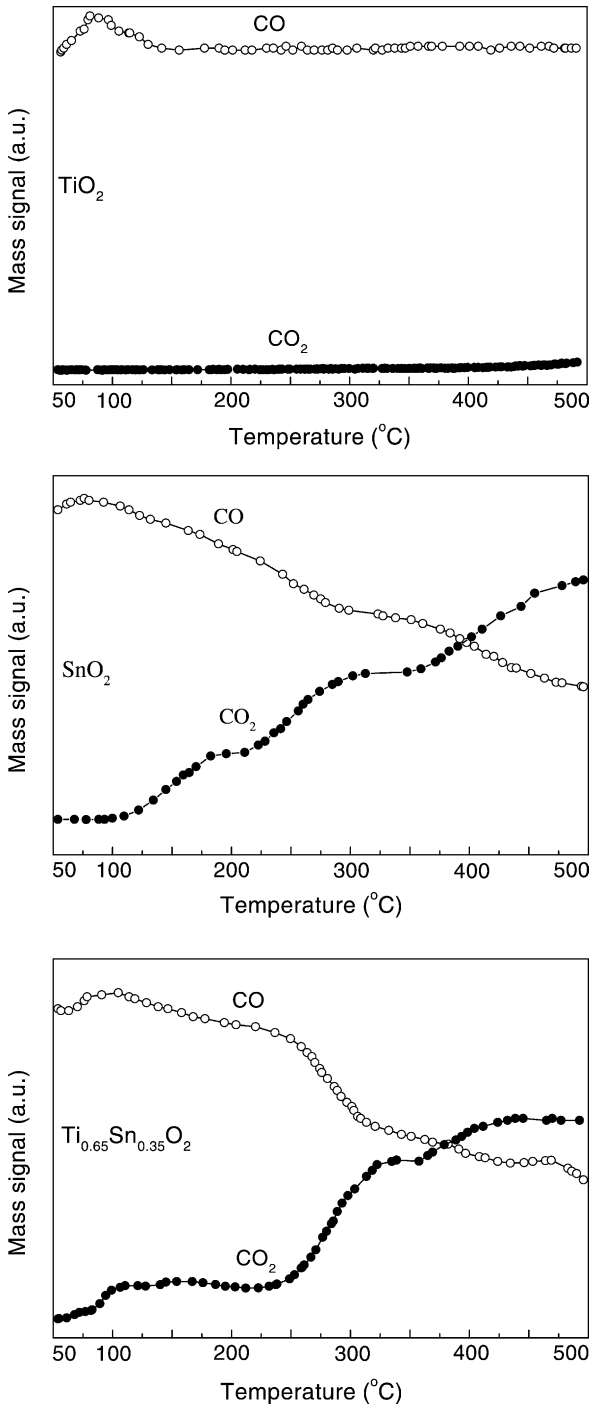

Fig. 6. Temperature programmed CO reduction of TiO_2 (anatase), SnO_2 and $Ti_{0.65}Sn_{0.35}O_2$ (200 mg, 4170 × 10^{-4} vol.% CO + Ar, 20 ml/min, 10 °C/min).

evident that there exists synergism for the reduction of SO_2. The catalytically active phase may be associated with the formation of Sn–O–Ti in the solid solutions, in conformity with the NMR data [54], which indicated that TiO_2–SnO_2 solid solutions form a rutile framework in which the cations are randomly distributed rather than distinct regions of TiO_2 and SnO_2. Kim et al. [10] has confirmed experimentally that the reduction of sulfur dioxide by carbon monoxide over rutile TiO_2 proceeds via redox mechanism:

$$\text{Cat} - [\,] + SO_2 \rightarrow \text{Cat} - O + SO \quad (1)$$

$$\text{Cat} - O + CO \rightarrow \text{Cat} - [\,] + CO_2 \quad (2)$$

$$\text{Cat} - [\,] + SO \rightarrow \text{Cat} - O + S \quad (3)$$

However, its activity is pretty low below 400 °C. The addition of only a small proportion of SnO_2 to the catalyst increases the activity drastically, especially below 350 °C. Meantime, adding a small amount of TiO_2 to the otherwise inactive SnO_2 improves the activity even more significantly.

As the atomic ratio of Sn/Ti shown, the catalyst surface is segregated of Sn after SO_2 + CO reactions. Combined with CO–TPR and previous results on SnO_2 [42], it is easy to think that SnO_2 plays an important role in the production of oxygen vacancies in the solid solutions. Thus, the above mentioned cooperative effort may be explained by the following enhanced redox mechanism: reaction (2) proceeds on Sn sites, so the reaction temperature can be greatly decreased compared with pure TiO_2; reactions (1) and (3) proceed on Ti sites, through which SO_2 is reduced to elemental sulfur. As the reaction temperature increased sufficiently high, for example, above 400 °C, the mobility of lattice oxygen on rutile TiO_2 is improved, CO is able to react with catalysts to generate oxygen vacancies. In this case, there exists little synergistic effort; the enhancing function of Sn is not evident either. For evidence, $Ti_{0.32}Sn_{0.68}O_2$ catalyst with most SnO_2 content showed the lowest SO_2 conversion among the catalysts after the reaction temperature exceeds 400 °C. On contrary, the SO_2 conversion of $Ti_{0.95}Sn_{0.05}O_2$ catalyst, which contains mainly rutile TiO_2, was lower at low temperatures (<400 °C), but much higher above 400 °C than that of $Ti_{0.32}Sn_{0.68}O_2$ catalyst (Fig. 1).

The important aspect of the enhanced redox mechanism lies in the fact that lattice oxygen can easily react with CO at low temperature to generate oxygen vacancies by the formation of TiO_2–SnO_2 solid solutions, which is otherwise impossible. This mechanism is different from the COS modified mechanism proposed in reference [10] or the remote control mechanism proposed in reference [8]. They both use sulfides as catalysts, which need an activation period at high temperatures in order to establish the synergistic state. In the present work, this state was already established after synthesis of the solid solutions. Titanium–tin solid solutions show, to our knowledge, the best activity at the lowest temperature towards SO_2 + CO reaction among the non-sulfide based catalysts up to now. However, the activity would decrease gradually with the increase of space velocity.

As confirmed by Sn 3d and S 2p spectra, tin sulfide was formed on the surface of used $Ti_{0.65}Sn_{0.35}O_2$ catalyst, showing the deposition of the reaction product, sulfur. Although, its amount is very low, the deposited sulfur on the catalyst surface will be shown a promoted effort on the catalytic activity during the reduction of NO by CO, and lay

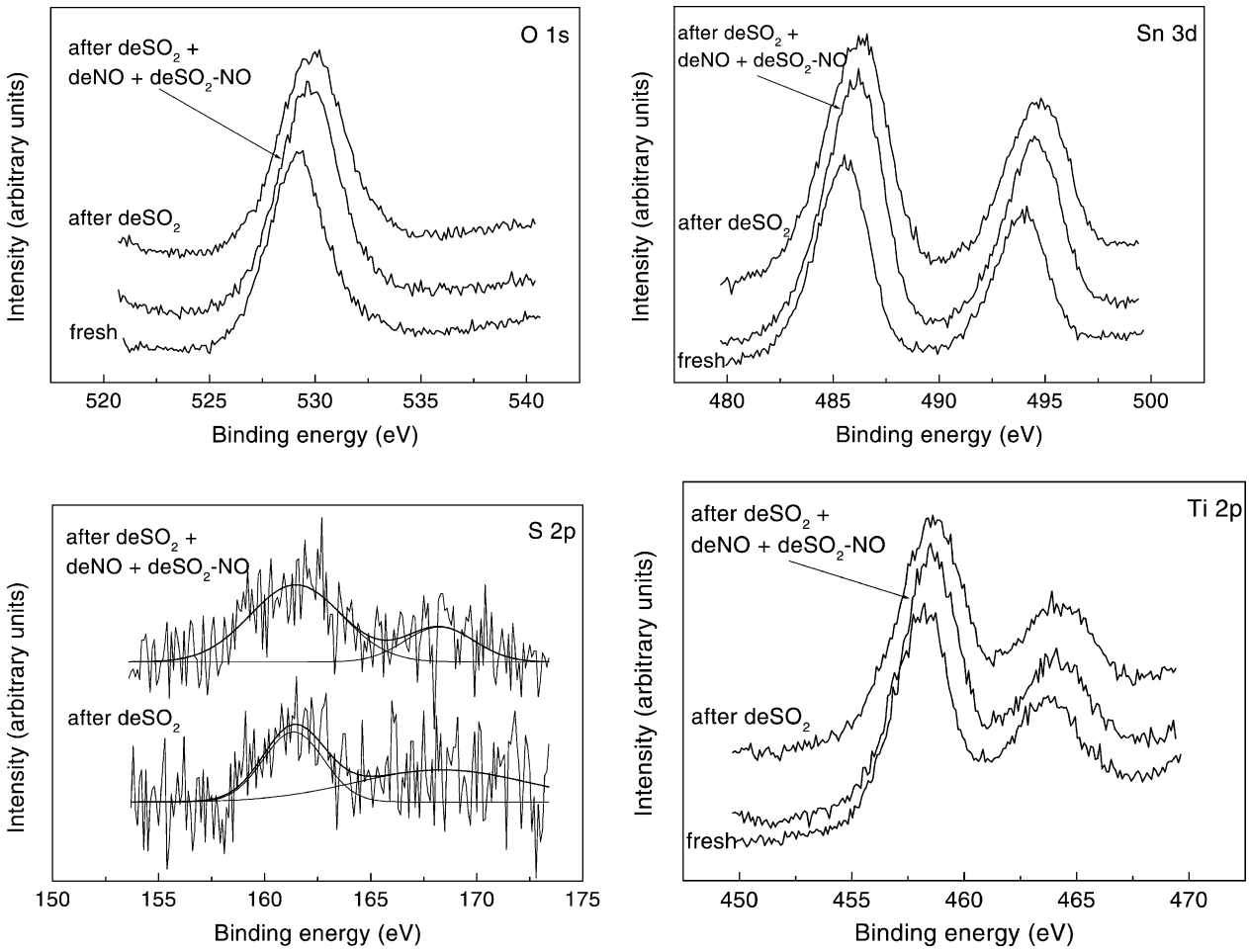

Fig. 7. XP spectra of fresh and used (after $deSO_2$ and after $deSO_2 + deNO + deSO_2 - NO$) $Ti_{0.65}Sn_{0.35}O_2$ catalysts.

the foundation for the effectively simultaneous reduction of SO_2 and NO by CO over the catalyst.

4.2. NO + CO reaction over fresh catalysts

As mentioned above, pure rutile TiO_2 shows negligible activity for the reduction of NO by CO below 400 °C. While pure SnO_2 prefers the oxidation of CO to the reduction of NO by CO. Actually, it does not show any activity towards the reduction of NO by CO below 350 °C. This has also been pointed by Solymosi and Kiss [55], who indicated that SnO_2 became completely inactive with the reduction time when the reaction temperature is below 360 °C, and a reproducible rate and conversion of NO were only observed above 360 °C.

Fig. 8 shows the NO conversion rate versus reaction time on fresh $Ti_{0.65}Sn_{0.35}O_2$ catalyst at 350 °C. The rate of NO reduction decreased with reaction time, which was similar to pure SnO_2. Therefore, it is reasonable to conclude that the activity of the fresh solid solutions at lower temperature is strongly related to SnO_2. However, even at elevated temperature the highest NO conversion over the fresh $Ti_{0.65}Sn_{0.35}O_2$ catalyst was only 46%, too less comparing with the same catalyst finishing $deSO_2$ reactions.

4.3. NO + CO reaction mechanism over catalysts after $deSO_2$ reactions

In order to understand the great differences of the NO + CO reaction on the solid solution catalysts before and after

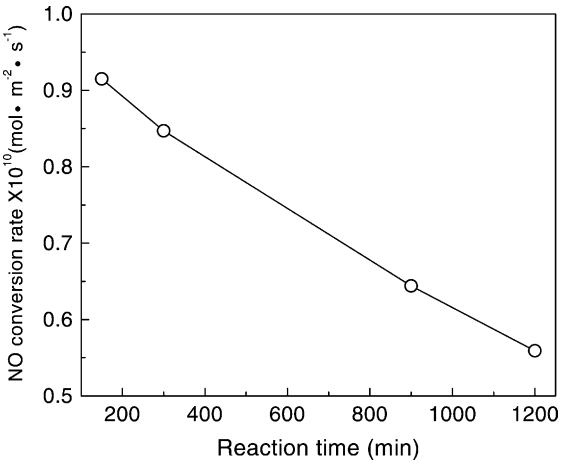

Fig. 8. NO conversion rate over the $Ti_{0.65}Sn_{0.35}O_2$ catalyst at 350 °C as a function of reaction time.

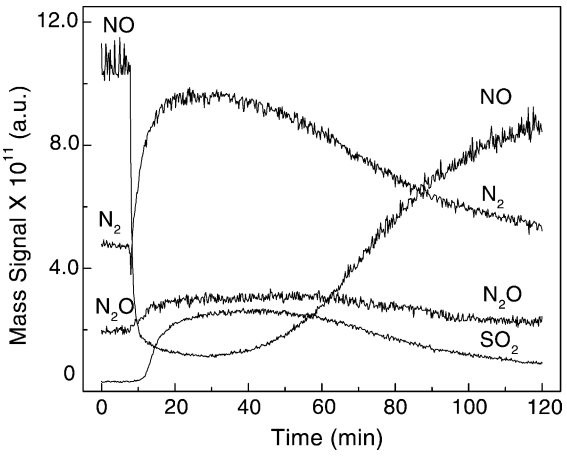

Fig. 9. Transient response curves obtained over the $Ti_{0.65}Sn_{0.35}O_2$ catalyst following deSO_2 reactions after switching from Ar to 2050×10^{-4} vol.% NO + Ar.

SO_2 + CO reactions, transient technique was employed. Fig. 9 shows the transient responses obtained at 350 °C on the $Ti_{0.65}Sn_{0.35}O_2$ catalyst following SO_2 + CO reactions after switching from Ar to Ar + 2050×10^{-4} vol.% NO. The instantaneous N_2 response curve concomitant with the formation of N_2O showed the solid solutions after deSO_2 reaction were active in the NO decomposition in the absence of CO in the gas phase. Similar results were also observed on the fresh catalyst (figure not shown here), but the great difference is that the sulfur-containing species, SO_2 (m/e = 64) was observed on the catalyst finishing SO_2 + CO reactions. The delayed response of SO_2 means that oxygen from NO decomposition was firstly taken up by the catalyst with high oxygen vacancies, and then reacted with the sulfur species on the catalyst surface. The catalytic activity of NO decomposition into N_2 and N_2O decreased with time, which results from the depletion of the surface sulfur species formed after SO_2 + CO reactions. Fig. 10 shows transient responses after introducing the reducing agent CO. It is obvious that SO_2 was only formed before 15 min, which could be thought as an activation period. As NO conversion was stable, the SO_2 response nearly returned to its initial level. It is also notable that negligible COS was produced during the whole test time, but given an enough long run, the catalyst could lose its activity owing to the formation of traces of unexpected SO_2 and COS by-products.

On the basis of high SO_2 conversion and selectivity to sulfur over the solid solutions, as described above, it is easy to explain the great activity for NO + CO reactions observed on those catalysts after deSO_2 reactions. The direct decomposition of NO was promoted in the presence of surface sulfide. From Fig. 9, it is evident that NO dissociated into N_2 through N_2O intermediate by the consumption of surface sulfur or the oxidation of the surface sulfide. Because less tin contained in the $Ti_{0.95}Sn_{0.05}O_2$ and $Ti_{0.88}Sn_{0.12}O_2$ catalysts, less tin sulfide were formed on catalyst surface, the promoting efforts on NO conversion were little. From Fig. 10, it is observed that the thus produced SO_2 can be in situ catalytically reduced to sulfur to regenerate tin sulfide forming a catalytic cycle. If the process was inhibited by high distribution of sulfide on catalyst surface as for the $Ti_{0.32}Sn_{0.68}O_2$ catalyst, the NO conversion would also decrease. Indeed, pure tin sulfide quickly lost activity. This mechanism has been verified by our previous work on cobalt sulfide and TiO_2-promoted cobalt sulfides [56].

4.4. SO_2 + NO + CO reaction

As mentioned in the introduction, the direct reduction of SO_2 by CO to sulfur has been reported in the absence of NO. At the same time, SO_2 is often thought to be the most important poison for flue gas cleanup application [23] as in automotive exhaust [15]. The efforts of NO on the reduction of SO_2 by CO and that of SO_2 on the reduction of NO by CO were both examined in this work as expressed in

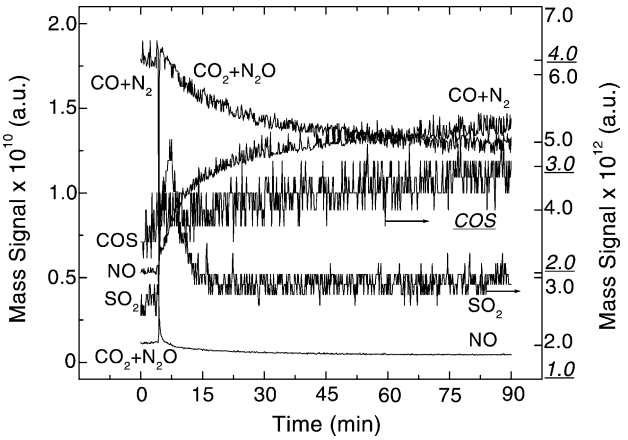

Fig. 10. Transient response curves obtained over the $Ti_{0.65}Sn_{0.35}O_2$ catalyst following deSO_2 reactions after switching from Ar to 1025×10^{-4} vol.% NO + 2085×10^{-4} vol.% CO + Ar.

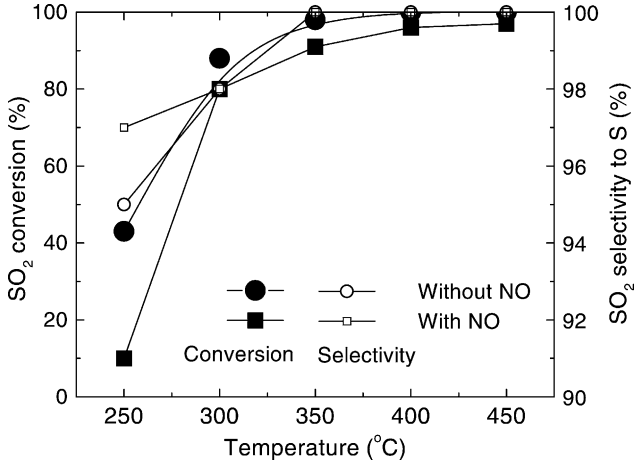

Fig. 11. NO effect on SO_2 conversions and selectivity to sulfur over the $Ti_{0.65}Sn_{0.35}O_2$ catalyst in the SO_2 + NO + CO reaction.

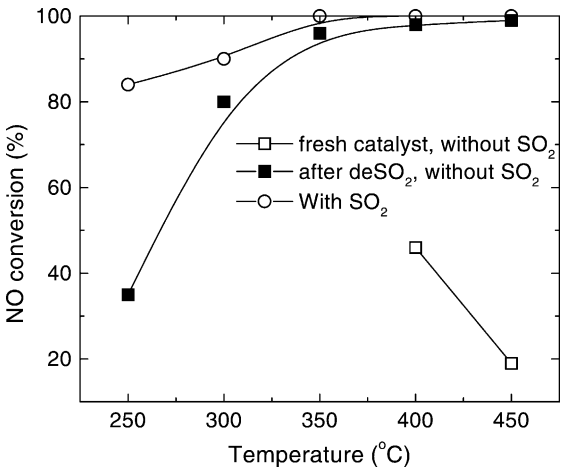

Fig. 12. SO_2 effect on NO conversion over the $Ti_{0.65}Sn_{0.35}O_2$ catalyst in the $SO_2 + NO + CO$ reaction.

the performance of simultaneous reduction of SO_2 and NO over the $Ti_{0.65}Sn_{0.35}O_2$ catalyst. Figs. 11 and 12 were partly redrawn from Figs. 1–3, which show the efforts of NO to SO_2 and vice versa. NO inhibits the reduction of SO_2 by CO to elemental sulfur, but only to a very small extent, and the inhibition becomes relatively less with increasing temperature. On the other hand, there is nearly no effect on SO_2 selectivity to sulfur. The decrease of SO_2 conversion in the presence of NO may be due to the extra SO_2 formed in the process of the simultaneous reduction of NO, which partly suppressed the reduction reaction of SO_2. In other words, NO adsorbed on tin sites where CO is to be adsorbed and oxidized. However, confirmation of this needs further work. Interestingly, as shown in Fig. 12, the addition of SO_2 did not poison the catalyst, but greatly promoted the NO conversion, and maintained the activity by supplement with elemental sulfur produced in the $SO_2 + CO$ reaction.

5. Conclusion

In the present study, it is revealed that TiO_2–SnO_2 solid solutions show very high activity for the SO_2+CO, NO+CO and $SO_2 + NO + CO$ reactions. Combined with the results of XRD, CO–TPR, XPS and transient MS techniques, the following conclusions can be drawn:

(1) TiO_2–SnO_2 solid solution catalysts exhibit outstanding activity and selectivity for the catalytic reduction of SO_2 to elemental sulfur by CO. The $Ti_{0.88}Sn_{0.12}O_2$ and $Ti_{0.65}Sn_{0.35}O_2$ catalysts without any pretreatment show a complete conversion of SO_2 towards elemental sulfur above 350 °C. The synergism between TiO_2 and SnO_2 is elucidated by an enhanced redox mechanism.

(2) Fresh TiO_2–SnO_2 solid solutions show either none or only a very low activity for the catalytic reduction of NO by CO. Most importantly, after $Ti_{0.65}Sn_{0.35}O_2$ and $Ti_{0.32}Sn_{0.68}O_2$ catalysts finished $SO_2 + CO$ reactions, an especially high activity with NO conversions of 96 and 90%, respectively, at 350 °C was achieved. This behavior is due to the formation of a sulfide species on the catalyst surface, which is confirmed by the XPS and transient techniques. A possible mechanism is that NO dissociated into N_2 through N_2O intermediate with the formation of SO_2 on the catalysts contaminated by surface sulfide species; the formed SO_2 can be in situ catalytically reduced to sulfur to regenerate the sulfide. The presence of SO_2 in the reaction stream is a necessity for a long-life catalyst.

(3) The simultaneous catalytic reduction of SO_2 and NO with CO was carried out over the $Ti_{0.65}Sn_{0.35}O_2$ catalyst. Although the activity for SO_2 removal was a little inhibited by the addition of NO, the NO conversions were dramatically increased by the presence of SO_2.

References

[1] J.N. Armor, Appl. Catal. B 1 (1992) 221.
[2] S.E. Khalafalla, E.F. Foester, L.A. Hass, Ind. Eng. Chem. Prod. Rev. Dev. 10 (1971) 133.
[3] D.B. Hibbert, A.C.C. Tseung, J. Chem. Soc., Faraday Trans. 74 (1978) 1981.
[4] J. Happel, M.A. Hnatow, L. Bajars, M. Kundrath, Ind. Eng. Chem. Prod. Res. Dev. 14 (1975) 154.
[5] D.B. Hibbert, R.H. Campbell, Appl. Catal. 41 (1988) 289.
[6] J.A. Bagilo, Ind. Eng. Chem. Prod. Res. Dev. 21 (1982) 38.
[7] J. Ma, M. Fang, N.T. Lau, Appl. Catal. A 150 (1997) 253.
[8] J. Ma, M. Fang, N.T. Lau, J. Catal. 158 (1996) 251.
[9] Y. Jiang, Y. Wu, Y. Xi, Y.T. Qian, J. Am. Ceram. Soc. 83 (2000) 2628.
[10] H. Kim, D.W. Park, H.C. Woo, J.S. Chung, Appl. Catal. B 19 (1998) 233.
[11] S.X. Zhuang, H. Magara, M. Yamazaki, Y. Takahashi, M. Yamada, Appl. Catal. B 24 (2000) 89.
[12] W. Liu, A.F. Sarofim, M. Flytzani-Stephanopoulos, Appl. Catal. B 4 (1994) 167.
[13] T. Zhu, L. Kundakovic, A. Dreher, M. Flytzani-Stephanopoulos, Catal. Today 50 (1999) 381.
[14] M. Flytzani-Stephanopoulos, T. Zhu, Y. Li, Catal. Today 62 (2000) 145.
[15] K.C. Taylor, Catal. Rev. Sci. Eng. 35 (1993) 457.
[16] M. Shelef, G.W. Graham, Catal. Rev. Sci. Eng. 36 (1994) 433.
[17] D.I. Kondarides, T. Chafik, X.E. Verykios, J. Catal. 191 (2000) 147.
[18] Y. Okamoto, T. Kubota, Y. Ohto, S. Nasu, J. Catal. 192 (2000) 412.
[19] Y. Hu, L. Dong, J. Wang, W. Ding, Y. Chen, J. Mol. Catal. A 162 (2000) 307.
[20] L. Simonot, F. Garin, G. Maire, Appl. Catal. B 11 (1997) 181.
[21] S.D. Peter, E. Garbowski, V. Perrichon, M. Primet, Catal. Lett. 70 (2000) 27.
[22] I. Spassova, M. Khristova, D. Panayotov, D. Mehandjiev, J. Catal. 185 (1999) 43.
[23] K. Arakawa, S. Matsuda, H. Kinoshita, Appl. Surf. Sci. 121/122 (1997) 382.
[24] H.S. Gandhi, M. Shelef, Appl. Catal. 77 (1991) 175.
[25] J. Blanco, A. Bahamonde, E. Alvarez, P. Avila, Catal. Today 42 (1998) 85.
[26] S. Kasaoka, E. Sasaoka, H. Iwasaki, Bull. Chem. Soc. Jpn. 62 (1989) 1226.
[27] S. Gao, N. Nakagawa, K. Kato, M. Inomata, F. Tsuchiya, Catal. Today 29 (1996) 165.

[28] S.M. Jeong, S.D. Kim, Ind. Eng. Chem. Res. 39 (2000) 1911.
[29] C.W. Quinlan, V.C. Okay, J.R. Kittrell, Ind. Eng. Chem. Process Des. Develop. 12 (1973) 359.
[30] V.N. Goetz, A. Sood, J.R. Kittrell, Ind. Eng. Chem. Prod. Res. Develop. 13 (1974) 110.
[31] A. Sood, J.R. Kittrell, Ind. Eng. Chem. Prod. Res. Develop. 13 (1974) 180.
[32] J.X. Ma, M. Fang, N.T. Lau, Catal. Lett. 62 (1999) 127.
[33] S.X. Zhuang, M. Yamazaki, K. Omata, Y. Takahashi, M. Yamada, Appl. Catal. B 31 (2001) 133.
[34] P.G. Harrison, C. Bailey, W. Azelee, J. Catal. 186 (1999) 147.
[35] Y. Teraoka, T. Harada, T. Iwasaki, T. Ikeda, S. Kagawa, Chem. Lett. (1993) 773.
[36] M.C. Kung, P.W. Park, D.W. Kim, H.H. Kung, J. Catal. 181 (1999) 1.
[37] P.W. Park, H.H. Kung, D.W. Kim, M.C. Kung, J. Catal. 184 (1999) 440.
[38] Y. Chen, Y. Jiang, W. Li, R. Jin, S. Tang, W. Hu, Catal. Today 50 (1999) 39.
[39] Z. Zhang, J. Ma, X. Yang, Acta Phys. Chim. Sin 17 (2001) 481.
[40] G. Xu, B. Wang, H. Suzuki, S. Gao, X. Ma, N. Nakagawa, K. Kato, J. Chem. Eng. Jpn. 32 (1999) 82.
[41] G. Sengupta, R.N. Chatterjee, G.C. Maity, B.J. Ansari, C.V.V. Satyanarayna, J. Colloid Interface Sci. 170 (1995) 215.
[42] J.F. Moulder, W.F. Stickle, P.E. Sobol, K.D. Bomben, Handbook of X-Ray Photoelectron Spectroscopy, Perkin-Elmer, 1992.
[43] W.H. Lee, H.C. Son, H.S. Moon, Y.I. Kim, S.H. Sung, J.Y. Kim, J.G. Lee, J.W. Park, J. Power Sources 89 (2000) 102.
[44] L.S. Price, I.P. Parkin, A.M.E. Hardy, R.J.H. Clark, Chem. Mater. 11 (1999) 1792.
[45] F. Berger, E. Beche, R. Berjoan, D. Klein, A. Chambaudet, Appl. Surf. Sci. 93 (1996) 9.
[46] J.P. Chen, R.T. Yang, J. Catal. 139 (1993) 277.
[47] T. Hirata, J. Am. Ceram. Soc. 83 (2000) 3205.
[48] V. Dusastre, D.E. Williams, J. Mater. Chem. 9 (1999) 445.
[49] M. Radecka, K. Zakrzewska, M. Rekas, Sens. Actuators B 47 (1998) 194.
[50] R.A. Eppler, J. Am. Ceram. Soc. 70 (1987) C–64.
[51] Y. Wu, Z. Zhao, Y. Liu, X. Yang, J. Mol. Catal. A 155 (2000) 89.
[52] M.J. Fuller, M.E. Warwick, J. Catal. 29 (1973) 441.
[53] G.M. Alikina, I.S. Sazonova, G.V. Glazneva, N.P. Keyer, React. Kinet. Catal. Lett. 3 (1975) 429.
[54] T.J. Bastow, L. Murgaski, M.E. Smith, H.J. Whitfield, Mater. Lett. 23 (1995) 117.
[55] F. Solymosi, J. Kiss, J. Catal. 41 (1976) 202.
[56] Z. Zhang, J. Ma, Z. Liu, S. Ren, X. Yang, Y. Kou, Chem. Lett. (2001) 464.